HHS Public Access

Author manuscript

Cancer Res. Author manuscript; available in PMC 2021 March 01.

Published in final edited form as:

Cancer Res. 2020 September 01; 80(17): 3519–3529. doi:10.1158/0008-5472.CAN-20-0216.

The synthetic small molecule FL3 combats intestinal tumorigenesis via Axin1-mediated inhibition of Wnt/beta-catenin signaling

Dakota N. Jackson[1], **Kibrom M. Alula**[4], **Yaritza Delgado-Deida**[4], **Redouane Tabti**[2], **Kevin Turner**[3], **Xuan Wang**[1], **K. Venuprasad**[3], **Rhonda F Souza**[1], **Laurent Désaubry**[2], **Arianne L. Theiss**[1,4,*]

[1]Department of Internal Medicine, Division of Gastroenterology, Baylor Scott & White Research Institute, Baylor University Medical Center, Dallas, TX

[2]Laboratory of Regenerative Nanomedicine (UMR 1260), INSERM-University of Strasbourg, Strasbourg, France

[3]University of Texas Southwestern Medical Center, College of Medicine, Dallas, TX

[4]Division of Gastroenterology and Hepatology, University of Colorado School of Medicine, Aurora, CO

Abstract

Colorectal cancer (CRC) exhibits aberrant activation of Wnt/beta-catenin signaling. Many inhibitors of the Wnt/beta-catenin pathway have been tested for Wnt-dependent cancers including CRC but are unsuccessful due to severe adverse reactions. FL3 is a synthetic derivative of natural products called flavaglines, which exhibit anti-inflammatory and cytoprotective properties in intestinal epithelial cells, but has not been previously tested in cell or pre-clinical models of intestinal tumorigenesis. In vitro studies suggest that flavaglines target Prohibitin 1 (PHB1) as a ligand, but this has not been established in the intestine. PHB1 is a highly conserved protein with diverse functions that depend on its post-translational modifications and subcellular localization. Here we demonstrate that FL3 combats intestinal tumorigenesis in the azoxymethane-dextran sodium sulfate and ApcMin/+ mouse models and in human CRC tumor organoids (tumoroids) by inhibiting Wnt/beta-catenin signaling via induction of Axin1 expression. FL3 exhibited no change in cell viability in normal intestinal epithelial cells or human matched-normal colonoids. FL3 response was diminished in CRC cell lines and human CRC tumoroids harboring a mutation at S45 of beta-catenin. PHB1 deficiency in mice or in human CRC tumoroids abolished FL3-induced expression of Axin1 and drove tumoroid death. In CRC cells, FL3 treatment blocked phosphorylation of PHB1 at Thr258, resulting in its nuclear translocation and binding to the Axin1

*To whom correspondence should be addressed: Arianne L. Theiss, Division of Gastroenterology and Hepatology, University of Colorado School of Medicine, 12700 East 19th Avenue , RC2 Campus Box: B158 HSC, Aurora, CO, arianne.theiss@cuanschutz.edu.

Author contributions

Study concept and design: RFS, LD, ALT. Acquisition of data: DNJ, KMA, YDD, RT, KT, ALT. Analysis and interpretation of data: DNJ, KV, RFS, ALT. Drafting the manuscript: DNJ, ALT. Critical revision of the manuscript for important intellectual content: RFS, KV, LD, ALT.

Conflict of interest

The authors declare no potential conflicts of interest.

promoter. These results suggest that FL3 inhibits Wnt/beta-catenin signaling via PHB1-dependent activation of Axin1. FL3 therefore represents a novel compound that combats Wnt pathway-dependent cancers such as CRC.

Graphical Abstract

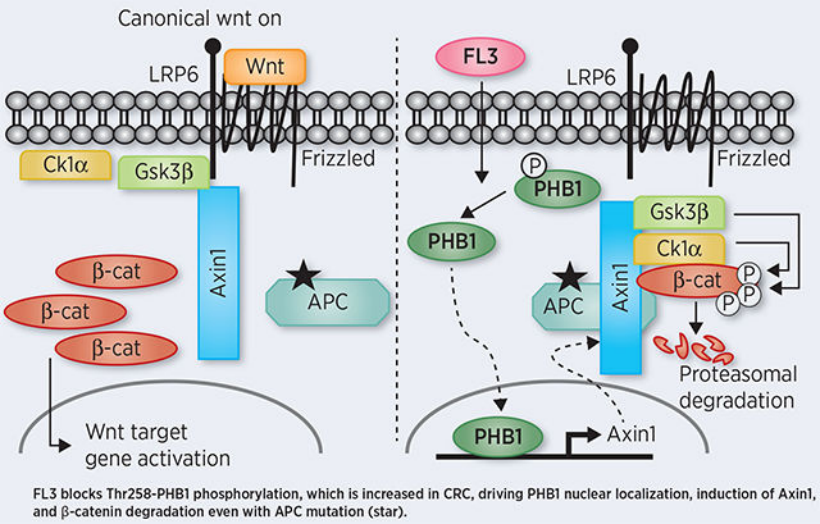

Keywords

colitis-associated cancer; colon cancer; natural compounds; β-catenin degradation complex; adenomatous polyposis coli

INTRODUCTION

Patients with chronic inflammatory bowel disease (IBD) of the colon have increased risk for colorectal cancer (CRC), accounting for nearly 10-15% of deaths in IBD patients (1). In these cases, CRC develops as a consequence of complications brought on by chronic colonic inflammation and is referred to as colitis-associated colorectal cancer (CA-CRC). Due to the well-established association of chronic inflammation with CRC development and malignant progression, use of anti-inflammatory agents to impede carcinogenesis is considered to be a highly effective strategy for CRC chemoprevention (2).

Flavaglines are a relatively new class of molecules derived from medicinal *Aglaia* (family *Meliaceae*) plants (3). Flavaglines have shown anti-cancer, anti-inflammatory, and cytoprotective activities *in vitro* (4). FL3 is a synthetic of the flavagline rocaglaol lacking the structural components linked to causing multidrug resistance and suboptimal pharmacokinetics, making it an ideal candidate for further investigation (3, 5). Previous studies demonstrated that FL3 at nanomolar concentrations exhibits cytoprotective effects in neurons (6), cardiomyocytes (7), and intestinal epithelial cells (8) and presents little toxicity to healthy cells (3, 9, 10). Our previous data suggest that FL3 combats inflammation using a mouse model of colitis, although we did not elucidate the mechanism of FL3 action (8). *In vitro* studies suggest that flavaglines target Prohibitins as ligands, but this has not been

established in the intestine (3). Prohibitin 1 (PHB1) is a highly conserved protein with diverse functions including regulation of cell cycle progression, apoptosis, and transcription depending on its post-translational modifications and subcellular localization (11). In intestinal epithelial cells, PHB1 is predominantly localized in the mitochondria, where it has been shown to be required for optimal activity of the electron transport chain (12–15).

Accumulation of select DNA mutations in tumor suppressors and oncogenes in colonic epithelial cells drives CRC, including CA-CRC, initiation and progression (16). The majority of CRC, including sporadic (up to 80%) and inflammation-induced (~50%), carry a genetic mutation in either *Adenomatous polyposis coli (APC)* or *CTNNB1* (encoding β-catenin), resulting in aberrant Wnt activation (17, 18). Although Wnt/β-catenin pathway mutations tend to occur late in CA-CRC development, studies suggest that activation of the Wnt/β-catenin pathway by numerous inflammatory signaling networks contribute to the onset and progression of CA-CRC (19). APC is a tumor suppressor due to its scaffolding role in the 'β-catenin destruction complex', which is a key node in regulating Wnt signaling (20). Axin1 and Axin2 are pivotal scaffold proteins that coordinate the assembly of APC, kinases CK1α and GSK3β, and their substrate β-catenin to facilitate the phosphorylation and subsequent proteasomal degradation of β-catenin under basal conditions. During Wnt stimulation, the destruction complex is inhibited, resulting in accumulation and nuclear translocation of β-catenin and transcriptional activation by binding to TCF/LEF sites on Wnt target genes that control proliferation, survival, and migration (21). Alterations in the *APC* gene found in CRC generate truncated mutants lacking all binding sites for Axin and abolish the formation of the β-catenin destruction complex. Current therapeutics cannot directly target APC. CRC mutations in *CTNNB1* render β-catenin resistant to phosphorylation and proteasomal degradation, leading to overexpression of β-catenin and Wnt target genes (22).

Many inhibitors of the Wnt/β-catenin pathway have been characterized, with some reaching early clinical trials (23). However, current Wnt-targeting compounds exhibit adverse reactions since Wnt signaling regulates homeostasis of many adult tissues, with the intestine being extremely vulnerable. For this reason, advancement of these compounds in clinical trials is impeded (24). Here, using human CRC cell lines with or without mutations in the *CTNNB1* gene, two mouse models of intestinal tumorigenesis, and mouse and human CRC tumoroids, we demonstrate that the targeting of PHB1 by FL3 provides a novel mechanism to inhibit aberrant Wnt signaling without intestinal toxicity.

MATERIALS AND METHODS

Description of histological dysplasia/adenoma scoring, SDS-PAGE and western immunoblot analysis, cell viability assay, MTT proliferation assay, cell migration assay, RNA isolation and quantitative real-time PCR analysis, TCF/LEF luciferase reporter, terminal deoxynucleotidyl transferase-mediated dUTP nick end labeling (TUNEL) staining, immunofluorescence and immunohistochemistry, chromatin immunoprecipitation, and RNAseq analysis is provided in the Supplementary Methods.

FL3 synthesis

FL3 was synthesized in our laboratory as previously described (25).

Animal models

All mice were grouped-housed in standard cages under a controlled temperature (25˚C) and photoperiod (12-hour light /dark cycle) and were allowed standard chow and tap water *ad libitum*. All experiments were approved by the Baylor Research Institute and the University of Colorado School of Medicine Institutional Animal Care and Use Committees. Experiments were performed with age- and gender-matched littermate mice.

AOM-DSS model: Age-matched male and female WT C57Bl/6 mice (Jackson Labs), $Phb1^{fl/fl}$ mice (C57Bl/6 genetic background), and $Phb1^{i\Delta IEC}$ mice (C57Bl/6 background and previously described (26)) at 8-weeks old were intraperitoneally (i.p.) injected with 7.6 mg/kg azoxymethane (AOM; Sigma-Aldrich) followed by 2 cycles of 3.0% (wt/vol) dextran sodium sulfate (DSS; molecular weight, 50,000; MP Biomedicals) in drinking water for 7 days followed by 14 or 21 days of recovery (regular drinking water). One day before and each day of DSS administration, mice were i.p. injected daily with 0.1 mg/kg FL3 or vehicle (100 μl volume). Upon sacrifice, colon was excised from the ileocecal junction to anus, cut open longitudinally, neoplasia number and size were quantitated using a dissecting microscope, and prepared for histological evaluation or biochemical analyses.

$Apc^{Min/+}$ model: Age-matched male and female $Apc^{Min/+}$ mice (Jackson Labs) and WT C57BL/6 littermates were i.p. injected with 0.1 mg/kg FL3 or vehicle (100 μl volume) twice per week starting at 15 weeks to 20 weeks. Upon sacrifice, the entire small intestine and colon were excised, cut open longitudinally, neoplasia number and size were quantitated using a dissecting microscope and prepared for histological evaluation or biochemical analyzes.

Human CRC and matched-normal specimens

Fresh, de-identified specimens of CRC, stage II and III, and matched-normal colon tissue were obtained from Baylor University Medical Center Pathology Department, which obtained written informed consent from patients undergoing resection surgery. The studies were conducted in accordance with the Belmont Report ethical principles and under Institutional IRB approval. Tissue specimens were stored in Advanced DMEM/F12 supplemented with penicillin/streptomycin until culturing which averaged 2-8 h later.

Human or mouse CRC tumoroid and colonoid culture

CRC tumoroids were derived from tumors digested in 125 μg/ml dispase type II, 75 U/ml collagenase type IX, and 0.2% Primocen. Colonoids were derived from isolated colonic crypts from mice or human specimens and cultured in Matrigel Basement Membrane Matrix (Corning) as previously described (27). Colonoids were grown in WENR media (Advanced DMEM/F12 supplemented with penicillin/streptomycin, 10 mM Hepes, 1× L-glutamine, 1× N2, 1× B27 (all from Life Technologies)), containing 100 ng/mL Wnt3α, 50 ng/mL recombinant epidermal growth factor (EGF), 500 ng/mL R-spondin1, and 100 ng/mL Noggin (all from R&D Systems). Tumoroids were grown in WNR medium (containing Wnt3α, Noggin, and R-spondin1) since CRC cells require no addition of growth factors such as EGF (27). Tumoroids and colonoids were grown for 7 d and treated with 10 or 50

nM FL3. For collection of protein lysates for Western blot, tumoroids were collected using Cultrex Organoid Harvesting Solution (Fisher Scientific) to remove Matrigel.

To determine whether human tumoroids exhibited deletion at S45 of β-catenin, genomic DNA was isolated from cultured tumoroids using the DNeasy Kit (Qiagen), 100 ng genomic DNA was amplified by PCR using the following primers: sense: 5′-CAATGGGTCATATCACAGATTCTT-3′ antisense: 5′-TCTCTTTTCTTCACCACAACATTT-3′, and the PCR products were gel-purified and sequenced.

For transfection of sgPHB1, human tumoroids grown in matrigel were trypsinized into single cells and Nucleofected with human Prohibitin 1 CRISPR/Cas9 KO Plasmid (sc-416271, Santa Cruz) and human Prohibitin 1 HDR Plasmid (sc-416271-HDR, Santa Cruz) using Hepatocyte Nucleofector Kit (VPL-1004, Lonza) for 72 h.

Cell culture

RKO (CRL-2577), HCT-116 (CCL-247), SW48, and IEC-6 cells were acquired from the American Type Culture Collection (ATCC) in 2017. Cells were cultured in 1X Dulbecco's modified Eagle's medium (DMEM) supplemented with 10% fetal bovine serum and 40 mg/L penicillin and 90 mg/L streptomycin. Cells were maintained in an incubator with 5% CO_2 at 37°C. All experiments were performed on RKO cells between passages 5 and 19, HCT-116 between passages 7 and 12, SW48 between passages 5 and 9, and IEC-6 between passages 19 and 26. All cell lines were verified to be mycoplasma-free using Genlantis MycoScope PCR Detection kit (Fisher Scientific) as recently as March 15, 2020 (RKO, HCT116, IEC-6) or April 7, 2020 (SW48).

To generate RKO cells stably expressing β-catenin harboring deletion of S45, RKO cells were transfected with Pcl-neo-β-catenin-Δ45 (Addgene) using Nucleofector T kit (Lonza). 48 h following transfection, transfected cells were selected with 1000 ug/mL of G418 (Geneticin; Gibco) for 3 to 5 weeks. Single clones were then isolated, maintained under 200 ug/mL G418 selection, and DNA sequenced for validation of exogenous β-catenin-Δ45 expression using the following primers: sense: 5′-ATGGCCATGGAACCAGACAG-3′ antisense: 5′-CTGAGAAAATCCCTGTTCCCAC-3′. Since these cell lines still express wild-type endogenous β-catenin, sequencing confirmed heterozygous S45 deletion. To knockdown Axin1 expression, RKO cells were Nucleofected with 20 μM of three pooled unique 27mer siRNA duplexes against Axin1 (SR305433; Origene) or 20 μM Stealth RNAi non-specific Negative Control Med GC (siNC; Invitrogen).

Statistical analysis

Data are presented as individual data points ± SEM. An unpaired two-tailed Student's *t* test was used for single comparisons, one-way ANOVA with Bonferroni post hoc test for multiple comparisons, and two-way ANOVA with Bonferroni post hoc test for assessing the combination of Axin1 knockdown and FL3 treatment (GraphPad Prism 8.0). For RNAseq analysis, genes were filtered for CPM ≥ 1 and differential gene expression was determined using R package DESeq2 (Bioconductor), $P < 0.05$, FDR ≤ 0.05, log2FC > 0.32. Ingenuity Pathway Analysis (Qiagen) identified significantly altered pathways.

RESULTS

FL3 decreases AOM-DSS-induced colonic tumorigenesis

To induce CA-CRC in mice, wild-type (WT) C57BL/6 mice were i.p. injected with AOM, followed by 2 cycles of DSS, consisting of 3.0% (wt/vol) DSS given in their drinking water for 7 days and 14 or 21 days recovery (regular drinking water). One day prior to and during each cycle of DSS, mice were i.p. injected daily with 0.1 mg/kg FL3 or vehicle. FL3 decreased the number and size of AOM-DSS-induced colonic neoplasia (Figure 1A and 1B) and decreased the histological occurrence of adenocarcinoma (Figure 1C and 1D), suggesting that FL3 prevents the progression of colitis to cancer. Importantly, the mice displayed no overt signs of toxicity or abnormal behavior from FL3 treatment. Colon tumoroids cultured from three independent AOM-DSS-treated mice and treated with FL3 at a low nanomolar concentration (10 nM) exhibited decreased viability and increased apoptosis (Figure 1E, 1F and Supplemental Figure S1A). RNA sequencing (RNAseq) analysis of AOM-DSS colon tumoroids treated with FL3 followed by Ingenuity Pathway Analysis identified Wnt/β-catenin signaling as the top canonical pathway altered by FL3 (P = 4.3E-04; Figure 1G). Of the genes identified by RNAseq, the expression of *Axin1* was most significantly altered by FL3 (P = 1.6E-08), followed by *Smek1* (P = 4.6E-07), *Tle4* (P = 2.8E-07), and *Klf4* (P = 2.3E-05). Western blotting confirmed increased Axin1 protein expression by FL3 as compared to negligible increases in Tle4, Smek1, or Klf4 (Supplemental Figure S1B). Significant increases in *Jun* (P = 8.9E-07), *ep300* (P = 4.6E-07) were also demonstrated by RNAseq, but this was not evident at the protein level (Supplemental Figure S1B). These results identify a potential role of Wnt/β-catenin inhibition in mediating anti-tumorigenic properties of FL3.

FL3 decreases transcriptional activation by β-catenin and protein expression in RKO and SW48 CRC cells

To determine whether FL3 inhibits the Wnt/β-catenin pathway, we utilized various human CRC cell lines with known *APC* and *CTNNB1* gene mutation status. 10 nM FL3 significantly decreased viability of RKO and SW48 cells but was not effective against HCT-116 cells or the non-transformed intestinal epithelial cell line IEC-6 (Supplemental Figure S2A). HCT-116 cells harbor a heterozygous deletion of S45 of β-catenin coupled with loss of heterozygosity (LOH), which is the site of phosphorylation by CK1α and the priming step necessary for phosphorylation of β-catenin at other sites that drive it to proteasomal degradation (22). Phosphorylation at S33 of β-catenin (mutant in SW48 cells) is dispensable if S45, S37, T41 are phosphorylated (22). FL3 induced cell death as measured by TUNEL staining and cleaved Caspase 3 expression in RKO and SW48 cells but not in HCT-116 or IEC6 cells (Supplemental Figure S2B–Supplemental Figure S2D). FL3 did not alter cell proliferation in any cell line tested and decreased migration of RKO and SW48 cells, but not HCT-116 cells (Supplemental Figure S3). These results suggest that FL3 therapeutic response to decrease cell viability and migration is dependent on β-catenin mutation status.

We next measured β-catenin activation and expression during FL3 treatment. Western blotting and immunofluorescent staining confirmed that 10 nM FL3 decreased β-catenin

protein expression in RKO and SW48 cells, but not in HCT-116 or IEC6 cells (Figure 2A and 2B). Human CRC cell lines were transfected with a TCF/LEF luciferase reporter plasmid to measure transcriptional activation by β-catenin and treated with FL3. 10 nM FL3 abolished relative luciferase expression to levels similar to negative control in RKO and SW48 cells, but in HCT-116 cells relative luciferase remained 6-fold higher than negative control (Figure 2C). Indeed, FL3 decreased expression of Wnt target genes in RKO cells (Figure 2D) and increased phosphorylation of β-catenin at S45 that inversely correlated with β-catenin degradation (Supplemental Figure S4A). Since HCT-116 cells harbor heterozygous G13D mutation of K-Ras in addition to heterozygous deletion of S45 of β-catenin, we stably-transfected RKO cells with a plasmid carrying the same HCT-116 S45-β-catenin deletion (RKO mut). RKO mut cells were no longer susceptible to FL3-induced β-catenin degradation (Supplemental Figure S4B and S4C) and cell death (Supplemental Figure S4D–F), suggesting that S45 of β-catenin is crucial for FL3 action. A cell viability comparison of FL3 to common CRC chemotherapeutic drugs 5-fluorouracil (5-FU), irinotecan, and oxaliplatin in a normal intestinal epithelial cell line (IEC6), a FL3-responsive CRC cell line (RKO), and a FL3-nonreponsive CRC cell line (HCT-116) demonstrates that FL3 did not decrease viability in IEC6 cells compared to 5-FU, irinotecan, or oxaliplatin (Supplemental Figure S5). 5-FU or oxaliplatin decreased cell viability in IEC-6 cells similarly to that in RKO or HCT-116 cells, suggesting equal toxicity by these drugs in normal intestinal epithelial cells and CRC cells (Supplemental Figure S5). Irinotecan did not alter viability compared to vehicle in any cell line tested.

FL3 inhibition of Wnt/β-catenin and induction of cell death in RKO cells is dependent on Axin1

Axin1 and Axin2 are pivotal scaffold proteins crucial for the formation of the β-catenin destruction complex. Axin is the least abundant component of the destruction complex due to proteasomal degradation by tankyrase and even small increases in Axin protein alters β-catenin (20). Unlike Axin2, which is a transcriptional target of β-catenin-dependent Wnt signaling, Axin1 is ubiquitously expressed and is classically thought of as a tumor suppressor protein (28). RKO cells with knockdown of Axin1 by 3 pooled siRNAs were resistant to FL3-induced β-catenin degradation (Figure 3A and 3B), β-catenin transcriptional activation (Figure 3C), and cell death (Figure 3D–F). These results suggest that FL3 anti-cancer mechanism in CRC is dependent on Axin1 degradation of β-catenin.

FL3 decreases intestinal tumorigenesis in the *Apc*$^{Min/+}$ mice

To determine whether FL3 is able to ameliorate colon tumorigenesis in a model of robust Wnt/β-catenin overexpression, *Apc*$^{Min/+}$ mice were administered 0.1 mg/kg FL3 or vehicle twice weekly from 15 to 20 weeks of age. FL3 significantly decreased the number and size of adenomas and severity of dysplasia in *Apc*$^{Min/+}$ mice (Figure 4A–C). This was associated with decreased β-catenin expression (Figure 4D) and increased cell death in adenomas (Figure 4E–G) but no change in cell proliferation (Supplemental Figure S6). Quantitation of TUNEL^{+} cells in non-tumor regions demonstrates that FL3 did not alter the number of apoptotic cells in normal crypts or villi *in vivo* (Figure 4F). These studies demonstrate that FL3 is sufficient to impact tumor growth in the absence of normal APC activity. WT mice injected with FL3 alongside *Apc*$^{Min/+}$ mice demonstrated normal gastrointestinal histology

including small intestinal villus length and small intestinal and colonic crypt length (Supplemental Figure S7).

FL3 decreases viability of human CRC tumoroids but not matched-normal colonoids

Historically, preclinical gastrointestinal translational research has relied on cell cultures that are of limited relevance to human physiology (27). These models often fail to predict human toxicity and/or efficacy (29). The establishment of 3D matrigel-based intestinal enteroid cultures in recent years provides a rapid and simple means to test toxicity and efficacy of pharmaceutical compounds in human specimens (27). To assess translational utility of FL3, tumoroids were cultured from human CRC specimens and colonoids from matched-normal tissue and treated with FL3. FL3 decreased viability of CRC tumoroids derived from 5 out of 6 patients, but did not affect cell viability in normal colonoids (Figure 5A and 5B). Sequencing analysis confirmed that tumoroids derived from Patient 3, which were resistant to FL3 treatment, harbored heterozygous S45 deletion of β-catenin, corroborating our results in HCT-116 cells. All other patients were wild-type at S45 of β-catenin.

PHB1 expression is required for FL3 anti-tumorigenic action in the colon

Mice with Villin-CreER^{T2} tamoxifen inducible deletion of *Phb1* from the intestinal epithelium (*Phb1*$^{i\Delta IEC}$) were recently described (30). We utilized this model to determine whether PHB1 is necessary for FL3 to combat colonic tumorigenesis. Since we have not observed spontaneous colonic neoplasia in *Phb1*$^{i\Delta IEC}$ mice up to 12 weeks following deletion of *Phb1*, we induced CA-CRC in *Phb1*$^{i\Delta IEC}$ and *Phb1*$^{fl/fl}$ control mice using AOM-DSS and cultured tumoroids. FL3 induced death of tumoroids derived from *Phb1*$^{fl/fl}$ mice, whereas FL3 had no effect on tumoroids derived from *Phb1*$^{i\Delta IEC}$ mice (Supplemental Figure S8A and S8B). Additionally, FL3 induction of Axin1 was absent in *Phb1* deficient tumoroids (Supplemental Figure S8C). We next selected human CRC tumoroids from a patient responsive to FL3 (Patient 1; Figure 5B) and targeted *PHB1* using CRISPR-Cas9 sgRNAs (Figure 5C). FL3 was ineffective to increase Axin1 expression (Figure 5C) and to decrease viability in *PHB1*-targeted human CRC tumoroids (Figure 5D). These data suggest that PHB1 is required for FL3 anti-tumor action in the colon. To demonstrate aberrant glycosylation in our tumoroid model compared to colonoids, which is an important feature of cancer cells (31), CRC tumoroids exhibited increased sialylated-Tn (a shortened glycan formed from incomplete synthesis of *O*-glycans common in cancer) and increased *N*-acetylglucosamine transferase (GnT-V) that is commonly upregulated in cancer (Figure 5E). These findings are important for the translational relevance of FL3 using CRC tumoroid models and are in agreement with previous reports demonstrating glycocalyx expression in intestinal and colonic organoids (32, 33).

The role of PHB1 in cancer depends upon the tumor type, with expression of PHB1 being reported as increased in CRC (34, 35). Dynamic partitioning of PHB1 between nuclear and cytoplasmic compartments of tumor cells has been shown to be signal-dependent and necessary for the induction of apoptosis (36). Compared to the non-transformed cell line IEC6, CRC cells exhibited increased phosphorylation of PHB1 at Thr258 (Figure 6A), a post-translational modification that induces mitochondrial localization of PHB1 in other types of cancer and correlates with enhanced proliferation, invasion, and metastasis (37, 38).

FL3 inhibited phosphorylation of PHB1 at Thr258 in CRC cells (Figure 6A) with a concomitant nuclear translocation of PHB1 in CRC cells but not in normal IECs (Figure 6B). In the nucleus, PHB1 has been shown to act as a co-regulator of transcription by interacting with various transcription factors such as p53, Rb, and E2F (3). A previous study identified PHB1 as a novel factor able to bind to the (TGYCC)n motif in the promoter of *p53-inducible gene 3 (PIG3)* (39). This motif is similar to the underlined portion of the p53 binding site (RRRCWWGYYY; R = A or G, W = A or T, Y = C or T) which repeats this motif with a 0-21 base pair spacer in-between. Using UCSC Genome Browser, the promoter regions of *Axin1*, *Smek1*, *Tle4*, and *Klf4* genes (the genes most significantly increased by FL3 in RNAseq analysis shown in Figure 1G) were searched for WGYYY or RGYYY motifs with or without a spacer. None were found in *Smek1*, *Tle4*, or *Klf4* promoters. However, the *Axin1* promoter contains the sequence 5′-GGCCTGGGCTTCGGCGCTCTGGCTCGGGCTCTGGCTC-3′ located -5668 to -5631 from the transcriptional start site (TSS) in the 5′UTR, which contains 5 RGYYY motifs (underlined), and we will refer to as putative PHB1 binding motif herein. ChIP assays demonstrated that PHB1 associates with this sequence in the *Axin1* promoter and that PHB1 binding is enriched by FL3 treatment in RKO cells (Figure 6C and 6D). Collectively, these results suggest a model for the *in vivo* anti-cancer mechanism of FL3 involving PHB1-induced Axin1 expression and β-catenin degradation.

DISCUSSION

FL3 is a novel pharmacologic agent, not previously tested in cell or pre-clinical models of intestinal tumorigenesis. Here, we provide proof-of-principle for fundamental mechanisms of FL3 to combat intestinal tumorigenesis without significant toxicity. Using an unbiased approach (RNAseq analysis), we identify inhibition of Wnt/β-catenin as the mechanism of FL3 anti-cancer activity dependent on PHB1 signaling. Importantly, we demonstrate translational utility of FL3 using human CRC tumoroids and matched-normal colonoids. FL3 provides a novel small molecule to combat cancers dependent on the Wnt pathway such CRC.

It is well established that genetic mutations in various genes are associated with different prognosis and response to CRC therapy. For instance, activating mutations in *K-Ras* render EGFR inhibition ineffective (40) and *tp53* mutation diminishes response to 5-fluorouracil (41). Response to FL3 was diminished in CRC cell lines harboring deletion of S45 of *CTNNB1* including HCT-116. HCT-116 cells harbor heterozygous G13D mutation of K-Ras in addition to heterozygous deletion of S45 of β-catenin. To determine which mutation diminishes FL3 response, stably-transfected RKO cells with a plasmid carrying the same HCT-116 S45-β-catenin deletion (RKO mut cells) were no longer susceptible to FL3-induced β-catenin degradation and cell death, suggesting that S45 of β-catenin is crucial for FL3 action. DNA sequencing revealed that the human CRC tumoroids unresponsive to FL3 (Patient 3) carried mutation at S45 of β-catenin. Collectively, these results suggest that FL3 anti-cancer action is dependent on degradation of β-catenin, requiring phosphorylation at S45.

FL3 decreased tumor number, size, and severity of dysplasia while increasing tumor cell death in two mouse models of intestinal tumorigenesis, one inflammation-induced model (AOM-DSS) and one sporadic model ($Apc^{Min/+}$ mice). FL3 efficacy in $Apc^{Min/+}$ mice demonstrates that FL3 is sufficient to combat tumorigenicity in a model driven by aberrant Wnt/β-catenin overexpression and in the absence of normal APC activity. This is especially important for the translational potential of FL3 since mutation in the *APC* gene is present in 49.5% of all CRC patients, a much higher percentage than mutation in the *CTNNB1* gene (4.99% of CRC patients) or *Axin1* gene (2.72% of CRC patients) (42), suggesting that the majority of CRC patients will likely respond to FL3 treatment based on *APC* and *CTNNB1* genetic mutation status. Heterogeneity of CA-CRC and sporadic CRC includes involvement of chromosomal instability (CIN), microsatellite instability (MSI), and promoter CpG island methylator phenotype (CIMP) (43–45). Future studies will further analyze these classifications in regards to FL3 response. Based on the CRC cell lines used in this study, HCT-116, RKO and SW48 are CIN^-/MSI-High, and therefore does not alter response to FL3. $CIMP^-$, which is the status of HCT-116 cells, could contribute to diminished FL3 responsiveness, whereas $CIMP^+$, which is the status of RKO and SW48, could be an important indicator of FL3 effectiveness. Future studies using other CIN^+/MSS/$CIMP^-$ cells such as Caco2 and HT29 will further elucidate FL3 response with these classifications.

The role of PHB1 in cancer depends upon the tumor type, with expression of PHB1 being reported as increased in CRC (34, 35). Dynamic partitioning of PHB1 between nuclear and cytoplasmic compartments of tumor cells has been shown to be signal-dependent and necessary for the induction of apoptosis in tumor cells (36). Although human PHB1 does not possess a mitochondrial targeting sequence, the N-terminal transmembrane domain of PHB1 (aa 2-24) targets it to the mitochondria where it is anchored to the inner mitochondrial membrane (46). At the C-terminus of PHB1, a leucine/isoleucine nuclear export sequence (NES) between aa 257-270 facilitates its export from the nucleus via CRM-1 export receptor to the cytoplasm (36). This specific structure of PHB1 allows active shuttling between the organelles. Previous studies have shown that phosphorylation of PHB1 at Thr258 enhances its mitochondrial localization in bladder and cervical cancer cells and is crucial to increased proliferation, invasion, and metastasis in these cancer cells (10, 37, 38). Here, we demonstrate that RKO, HCT-116, and SW48 CRC cells exhibit increased phosphorylation of PHB1 at Thr258, which is inhibited by FL3. Nuclear localization of PHB1 is induced by FL3 treatment in RKO CRC cells but not in non-transformed IEC6 cells. We show by ChIP that PHB1 binding to the 5′UTR of the *Axin1* gene is increased by FL3 in RKO CRC cells and that PHB1 deficiency in mouse and human CRC tumoroids abolishes FL3-induced Axin1 expression and cell death. These results suggest that, FL3 is an inhibitor of Wnt/β-catenin via blockade of PHB1 phosphorylation at Thr258 and subsequent PHB1 nuclear translocation where it induces transcription of Axin1, the core molecule and limiting component of the β-catenin degradation complex. PHB1 was shown to inhibit Wnt signaling in murine liver and human hepatocellular carcinoma cells via regulation of the transcription factor E2F1 (47). Interestingly, similar to FL3, other Axin1 stabilizers that act via tankyrase inhibition have been shown to impact tumorigenesis in the absence of normal APC activity (48). The tight control Axin1 expression exerts on the β-catenin destruction complex is a property currently being exploited in the development of novel therapeutics for Wnt-driven

cancers (20) and our results suggest that FL3 at low nanomolar concentrations upregulates Axin1 expression. We admit that PHB1 regulates multiple signaling pathways dependent on cell type studied, post-translational modifications of PHB1, and subcellular localization of PHB1. As examples, PHB1 can interact with C-RAF, Akt, IKK, and Stat3 (49). Given our unbiased RNAseq data implicating FL3 inhibition of Wnt/β-catenin signaling in CRC, we currently focused on this pathway. Future studies will elucidate the role of other known PHB1 signaling pathways in FL3 anti-tumorigenic properties in CRC.

Polymorphisms of the *PHB1* gene have been linked to gastric, breast, ovarian, and skin cancers but it remains unknown whether these genetic alterations affect PHB1 post-translational modifications or function (50). Our results elucidating FL3 mechanism via PHB1 action may provide an ability to stratify CRC patients by those who are most likely to respond to FL3 treatment (those with high p-Thr258-PHB1 expression and absence of S45 β-catenin mutation). FL3 treatment of non-transformed cells alongside CRC cells and CRC tumoroids, as well as no change by FL3 treatment in the number of TUNEL+ cells in normal crypts or villi *in vivo* suggests that FL3 lacks toxicity in normal intestinal epithelial cells. We propose that the targeting of PHB1 by FL3 provides a novel mechanism to inhibit Wnt signaling without intestinal toxicity since PHB1 nuclear shuttling response to FL3 is specific to CRC cells. Although many inhibitors of the Wnt/β-catenin pathway have been characterized with some reaching early clinical trials (23), these compounds exhibit significant adverse reactions given the role of Wnt signaling in maintaining homeostasis of many adult tissues, particularly the intestine. As examples, Wnt pathway inhibitors XAV939 and LGK974 result in severe intestinal toxicity in mice and OMP18R5 (Vantictumab) induces abdominal pain and diarrhea in patients preventing advancement in clinical trials (23). FL3 provides a novel small molecule Wnt/β-catenin inhibitor presenting little toxicity to healthy intestinal epithelial cells, as shown previously in other healthy cell types (3, 9, 10).

Our study defines a link between FL3, PHB1, and Wnt/β-catenin inhibition, which is a key pathway mediating intestinal carcinogenesis. These results provide important insight in the nuclear trafficking of PHB1 and its contribution to tumor death dependent on cellular localization and post-transcriptional modifications. We provide the first identification of *in vivo* molecular targets of FL3 and specifically identify a novel role of PHB1 in regulating Axin1 levels. FL3 provides a novel small molecule inhibitor of β-catenin via upregulation of Axin1 expression as a potential therapeutic for Wnt pathway-driven cancers such as CRC. Future studies are poised to build the pre-clinical biosafety profile of FL3 and test the role of FL3 as a sensitizing agent in chemoresistant CRC cell lines.

Supplementary Material

Refer to Web version on PubMed Central for supplementary material.

Acknowledgments

We thank Dr. Xiaofang Huo and Dr. Qiuyang Zhang for providing key antibodies, Jie Han and Masha Sorouri for technical assistance, Beth Cook for histology processing, Cynthia Smitherman for RNAseq analysis, and Jinghua Gu for biostatistical support (Baylor Scott & White Research Institute). This work was supported by National

Institutes of Health grants R01-DK117001 (ALT) and Litwin IBD Pioneers Crohn's Colitis Foundation 301869 (ALT).

Financial support

This work was supported by National Institutes of Health grants R01-DK117001 (ALT) and Litwin IBD Pioneers Crohn's Colitis Foundation 301869 (ALT).

Abbreviations:

APC	adenomatous polyposis coli
AOM	azoxymethane
CA-CRC	colitis-associated cancer
CRC	colorectal cancer
DSS	dextran sodium sulfate
IBD	inflammatory bowel disease
PHB1	Prohibitin 1
WT	wild-type

References

1. Mattar MC, Lough D, Pishvaian MJ, Charabaty A. Current management of inflammatory bowel disease and colorectal cancer. Gastrointest Cancer Res 2011;4:53–61. [PubMed: 21673876]
2. Fajardo AM, Piazza GA. Chemoprevention in gastrointestinal physiology and disease. Anti-inflammatory approaches for colorectal cancer chemoprevention. American journal of physiology Gastrointestinal and liver physiology 2015;309:G59–70. [PubMed: 26021807]
3. Thuaud F, Ribeiro N, Nebigil CG, Desaubry L. Prohibitin ligands in cell death and survival: mode of action and therapeutic potential. Chem Biol 2013;20:316–31. [PubMed: 23521790]
4. Li-Weber M Molecular mechanisms and anti-cancer aspects of the medicinal phytochemicals rocaglamides (=flavaglines). Int J Cancer 2015;137:1791–9. [PubMed: 24895251]
5. Liu T, Nair SJ, Lescarbeau A, Belani J, Peluso S, Conley J, et al. Synthetic silvestrol analogues as potent and selective protein synthesis inhibitors. Journal of medicinal chemistry 2012;55:8859–78. [PubMed: 23025805]
6. Fahrig T, Gerlach I, Horvath E. A synthetic derivative of the natural product rocaglaol is a potent inhibitor of cytokine-mediated signaling and shows neuroprotective activity in vitro and in animal models of Parkinson's disease and traumatic brain injury. Mol Pharmacol 2005;67:1544–55. [PubMed: 15716464]
7. Bernard Y, Ribeiro N, Thuaud F, Turkeri G, Dirr R, Boulberdaa M, et al. Flavaglines alleviate doxorubicin cardiotoxicity: implication of Hsp27. PLoS One 2011;6:e25302. [PubMed: 22065986]
8. Han J, Zhao Q, Basmadjian C, Desaubry L, Theiss AL. Flavaglines Ameliorate Experimental Colitis and Protect Against Intestinal Epithelial Cell Apoptosis and Mitochondrial Dysfunction. Inflammatory bowel diseases 2016;22:55–67. [PubMed: 26398710]
9. Qureshi R, Yildirim O, Gasser A, Basmadjian C, Zhao Q, Wilmet JP, et al. FL3, a Synthetic Flavagline and Ligand of Prohibitins, Protects Cardiomyocytes via STAT3 from Doxorubicin Toxicity. PLoS One 2015;10:e0141826. [PubMed: 26536361]
10. Yuan G, Chen X, Liu Z, Wei W, Shu Q, Abou-Hamdan H, et al. Flavagline analog FL3 induces cell cycle arrest in urothelial carcinoma cell of the bladder by inhibiting the Akt/PHB interaction to activate the GADD45alpha pathway. J Exp Clin Cancer Res 2018;37:21. [PubMed: 29415747]

11. Basmadjian C, Thuaud F, Ribeiro N, Desaubry L. Flavaglines: potent anticancer drugs that target prohibitins and the helicase eIF4A. Future Med Chem 2013;5:2185–97. [PubMed: 24261894]
12. Bourges I, Ramus C, Mousson de Camaret B, Beugnot R, Remacle C, Cardol P, et al. Structural organization of mitochondrial human complex I: role of the ND4 and ND5 mitochondria-encoded subunits and interaction with prohibitin. Biochem J 2004;383:491–9. [PubMed: 15250827]
13. Hsieh SY, Shih TC, Yeh CY, Lin CJ, Chou YY, Lee YS. Comparative proteomic studies on the pathogenesis of human ulcerative colitis. Proteomics 2006;6:5322–31. [PubMed: 16947118]
14. Theiss AL, Idell RD, Srinivasan S, Klapproth JM, Jones DP, Merlin D, et al. Prohibitin protects against oxidative stress in intestinal epithelial cells. Faseb J 2007;21:197–206. [PubMed: 17135366]
15. Tsutsumi T, Matsuda M, Aizaki H, Moriya K, Miyoshi H, Fujie H, et al. Proteomics analysis of mitochondrial proteins reveals overexpression of a mitochondrial protein chaperon, prohibitin, in cells expressing hepatitis C virus core protein. Hepatology 2009;50:378–86. [PubMed: 19591124]
16. Van Der Kraak L, Gros P, Beauchemin N. Colitis-associated colon cancer: Is it in your genes? World journal of gastroenterology 2015;21:11688–99. [PubMed: 26556996]
17. Conlin A, Smith G, Carey FA, Wolf CR, Steele RJ. The prognostic significance of K-ras, p53, and APC mutations in colorectal carcinoma. Gut 2005;54:1283–6. [PubMed: 15843421]
18. Yamauchi M, Morikawa T, Kuchiba A, Imamura Y, Qian ZR, Nishihara R, et al. Assessment of colorectal cancer molecular features along bowel subsites challenges the conception of distinct dichotomy of proximal versus distal colorectum. Gut 2012;61:847–54. [PubMed: 22427238]
19. Koch S Extrinsic control of Wnt signaling in the intestine. Differentiation 2017;97:1–8. [PubMed: 28802143]
20. Wang Z, Tacchelly-Benites O, Yang E, Thorne CA, Nojima H, Lee E, et al. Wnt/Wingless Pathway Activation Is Promoted by a Critical Threshold of Axin Maintained by the Tumor Suppressor APC and the ADP-Ribose Polymerase Tankyrase. Genetics 2016;203:269–81. [PubMed: 26975665]
21. Daugherty RL, Gottardi CJ. Phospho-regulation of Beta-catenin adhesion and signaling functions. Physiology (Bethesda) 2007;22:303–9. [PubMed: 17928543]
22. Tortelote GG, Reis RR, de Almeida Mendes F, Abreu JG. Complexity of the Wnt/betacatenin pathway: Searching for an activation model. Cell Signal 2017;40:30–43. [PubMed: 28844868]
23. Krishnamurthy N, Kurzrock R. Targeting the Wnt/beta-catenin pathway in cancer: Update on effectors and inhibitors. Cancer Treat Rev 2018;62:50–60. [PubMed: 29169144]
24. Shang S, Hua F, Hu ZW. The regulation of beta-catenin activity and function in cancer: therapeutic opportunities. Oncotarget 2017;8:33972–89. [PubMed: 28430641]
25. Thuaud F, Bernard Y, Turkeri G, Dirr R, Aubert G, Cresteil T, et al. Synthetic analogue of rocaglaol displays a potent and selective cytotoxicity in cancer cells: involvement of apoptosis inducing factor and caspase-12. Journal of medicinal chemistry 2009;52:5176–87. [PubMed: 19655762]
26. Jackson DN, Panopoulos M, Neumann WL, Turner K, Cantarel BL, Thompson-Snipes L, et al. Mitochondrial dysfunction during loss of Prohibitin 1 triggers Paneth cell defects and ileitis. Gut 2020:Resubmission.
27. Sato T, Stange DE, Ferrante M, Vries RG, Van Es JH, Van den Brink S, et al. Long-term expansion of epithelial organoids from human colon, adenoma, adenocarcinoma, and Barrett's epithelium. Gastroenterology 2011;141:1762–72. [PubMed: 21889923]
28. Mazzoni SM, Fearon ER. AXIN1 and AXIN2 variants in gastrointestinal cancers. Cancer Lett 2014;355:1–8. [PubMed: 25236910]
29. Howell JC, Wells JM. Generating intestinal tissue from stem cells: potential for research and therapy. Regenerative medicine 2011;6:743–55. [PubMed: 22050526]
30. Jackson DN, Panopoulos M, Neumann WL, Turner K, Cantarel BL, Thompson-Snipes L, et al. Mitochondrial dysfunction during loss of prohibitin 1 triggers Paneth cell defects and ileitis. Gut 2020.
31. Kang H, Wu Q, Sun A, Liu X, Fan Y, Deng X. Cancer Cell Glycocalyx and Its Significance in Cancer Progression. Int J Mol Sci 2018;19.
32. Fujii M, Clevers H, Sato T. Modeling Human Digestive Diseases With CRISPR-Cas9-Modified Organoids. Gastroenterology 2019;156:562–76. [PubMed: 30476497]

33. Rouhanifard SH, Lopez Aguilar A, Meng L, Moremen KW, Wu P. Engineered Glycocalyx Regulates Stem Cell Proliferation in Murine Crypt Organoids. Cell Chem Biol 2018;25:439–46 e5. [PubMed: 29429899]
34. Chen YW, Chou HC, Lyu PC, Yin HS, Huang FL, Chang WS, et al. Mitochondrial proteomics analysis of tumorigenic and metastatic breast cancer markers. Functional & integrative genomics 2011;11:225–39. [PubMed: 21246238]
35. Hammoudi A, Song F, Reed KR, Jenkins RE, Meniel VS, Watson AJ, et al. Proteomic profiling of a mouse model of acute intestinal Apc deletion leads to identification of potential novel biomarkers of human colorectal cancer (CRC). Biochemical and biophysical research communications 2013;440:364–70. [PubMed: 23998936]
36. Rastogi S, Joshi B, Fusaro G, Chellappan S. Camptothecin induces nuclear export of prohibitin preferentially in transformed cells through a CRM-1-dependent mechanism. J Biol Chem 2006;281:2951–9. [PubMed: 16319068]
37. Chiu CF, Ho MY, Peng JM, Hung SW, Lee WH, Liang CM, et al. Raf activation by Ras and promotion of cellular metastasis require phosphorylation of prohibitin in the raft domain of the plasma membrane. Oncogene 2013;32:777–87. [PubMed: 22410782]
38. Jiang L, Dong P, Zhang Z, Li C, Li Y, Liao Y, et al. Akt phosphorylates Prohibitin 1 to mediate its mitochondrial localization and promote proliferation of bladder cancer cells. Cell death & disease 2015;6:e1660. [PubMed: 25719244]
39. Guan X, Liu Z, Wang L, Johnson DG, Wei Q. Identification of prohibitin and prohibiton as novel factors binding to the p53 induced gene 3 (PIG3) promoter (TGYCC)(15) motif. Biochemical and biophysical research communications 2014;443:1239–44. [PubMed: 24388982]
40. Shi C, Washington K. Molecular testing in colorectal cancer: diagnosis of Lynch syndrome and personalized cancer medicine. American journal of clinical pathology 2012;137:847–59. [PubMed: 22586043]
41. Iacopetta B TP53 mutation in colorectal cancer. Human mutation 2003;21:271–6. [PubMed: 12619112]
42. Consortium APG. AACR Project GENIE: Powering Precision Medicine through an International Consortium. Cancer Discov 2017;7:818–31. [PubMed: 28572459]
43. Habermann JK, Upender MB, Roblick UJ, Kruger S, Freitag S, Blegen H, et al. Pronounced chromosomal instability and multiple gene amplifications characterize ulcerative colitis-associated colorectal carcinomas. Cancer Genet Cytogenet 2003;147:9–17. [PubMed: 14580765]
44. Scarpa M, Scarpa M, Castagliuolo I, Erroi F, Kotsafti A, Basato S, et al. Aberrant gene methylation in non-neoplastic mucosa as a predictive marker of ulcerative colitis-associated CRC. Oncotarget 2016;7:10322–31. [PubMed: 26862732]
45. Shivakumar BM, Rotti H, Vasudevan TG, Balakrishnan A, Chakrabarty S, Bhat G, et al. Copy number variations are progressively associated with the pathogenesis of colorectal cancer in ulcerative colitis. World journal of gastroenterology 2015;21:616–22. [PubMed: 25605985]
46. Peng YT, Chen P, Ouyang RY, Song L. Multifaceted role of prohibitin in cell survival and apoptosis. Apoptosis : an international journal on programmed cell death 2015;20:1135–49. [PubMed: 26091791]
47. Mavila N, Tang Y, Berlind J, Ramani K, Wang J, Mato JM, et al. Prohibitin 1 Acts As a Negative Regulator of Wingless/Integrated-Beta-Catenin Signaling in Murine Liver and Human Liver Cancer Cells. Hepatol Commun 2018;2:1583–600. [PubMed: 30556043]
48. Lau T, Chan E, Callow M, Waaler J, Boggs J, Blake RA, et al. A novel tankyrase small-molecule inhibitor suppresses APC mutation-driven colorectal tumor growth. Cancer Res 2013;73:3132–44. [PubMed: 23539443]
49. Wang D, Tabti R, Elderwish S, Abou-Hamdan H, Djehal A, Yu P, et al. Prohibitin ligands: a growing armamentarium to tackle cancers, osteoporosis, inflammatory, cardiac and neurological diseases. Cell Mol Life Sci 2020.
50. Chowdhury D, Kumar D, Sarma P, Tangutur AD, Bhadra MP. PHB in Cardiovascular and Other Diseases: Present Knowledge and Implications. Curr Drug Targets 2017;18:1836–51. [PubMed: 27557820]

SIGNIFICANCE

Targeting of PHB1 by FL3 provides a novel mechanism to combat Wnt-driven cancers with limited intestinal toxicity.

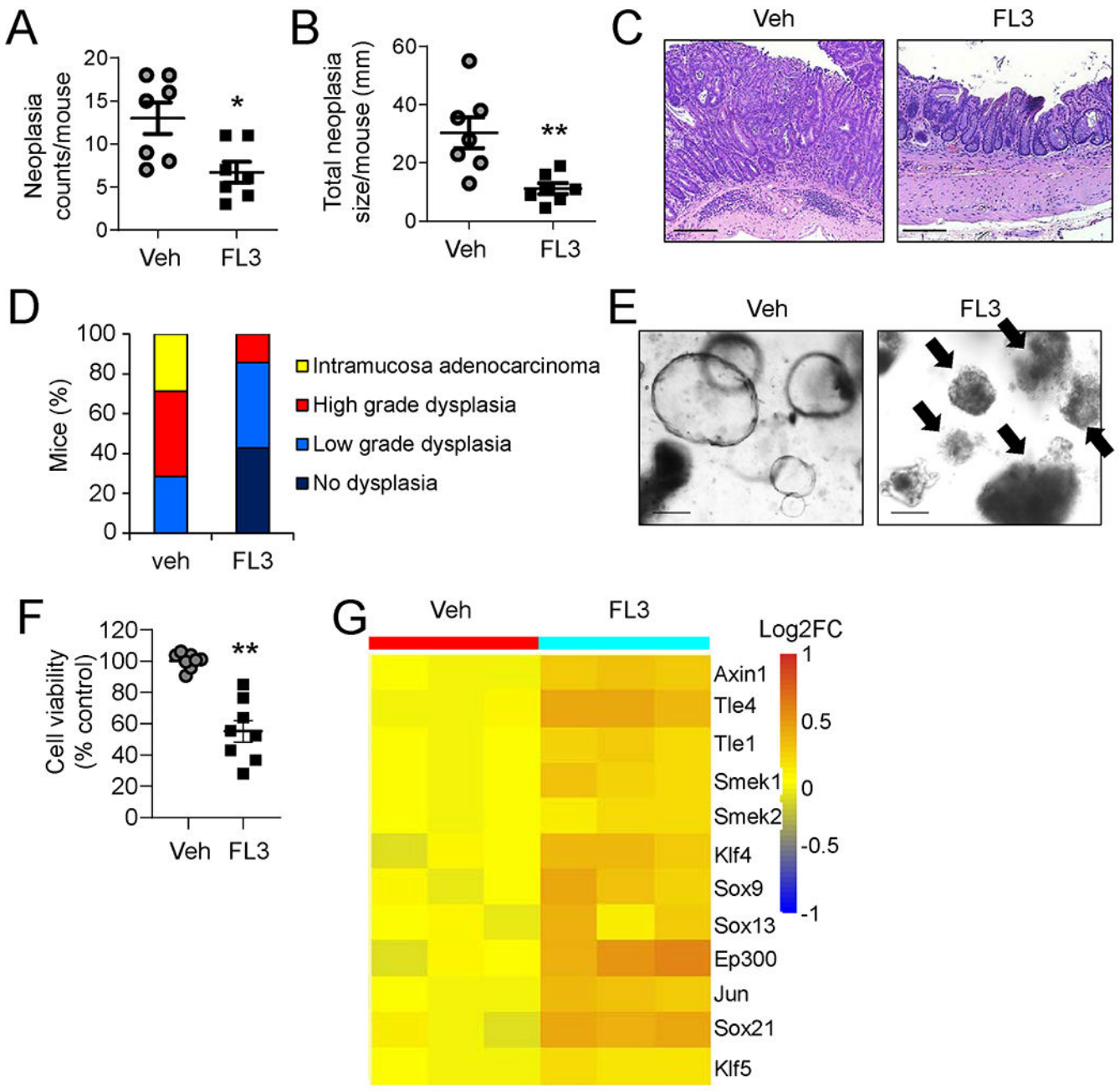

Figure 1. FL3 decreases AOM-DSS-induced colonic tumorigenesis.

One day prior to and during each cycle of DSS, mice were i.p. injected daily with 0.1 mg/kg FL3 or vehicle. (A) Average neoplasia counts per mouse. (B) Average neoplasia size per mouse. (C) H&E staining of colon histology from AOM-DSS-treated mice. Scale bars: 250 μm. (D) Percentage of mice displaying highest extent of dysplasia. n = 7 per group. (E-G) Colonic tumoroids were cultured from AOM-DSS-induced tumors from 3 independent mice and grown in matrigel for 7 days. Tumoroids were then treated with 10 nM FL3 or vehicle. (E) Morphological changes in dead tumoroids treated with FL3 for 16 h (arrows). Scale bars: 100 μm. (F) Cell viability measured by LDH release after 16 h FL3 treatment. n = 8

per group. (G) Heat map of genes implicated in regulating Wnt/β-catenin signaling identified by RNAseq analysis using total RNA from tumoroids treated with FL3 for 2 h. $^{**}P < 0.01$, $^{*}P < 0.05$ by unpaired, two-tailed Student's *t* test.

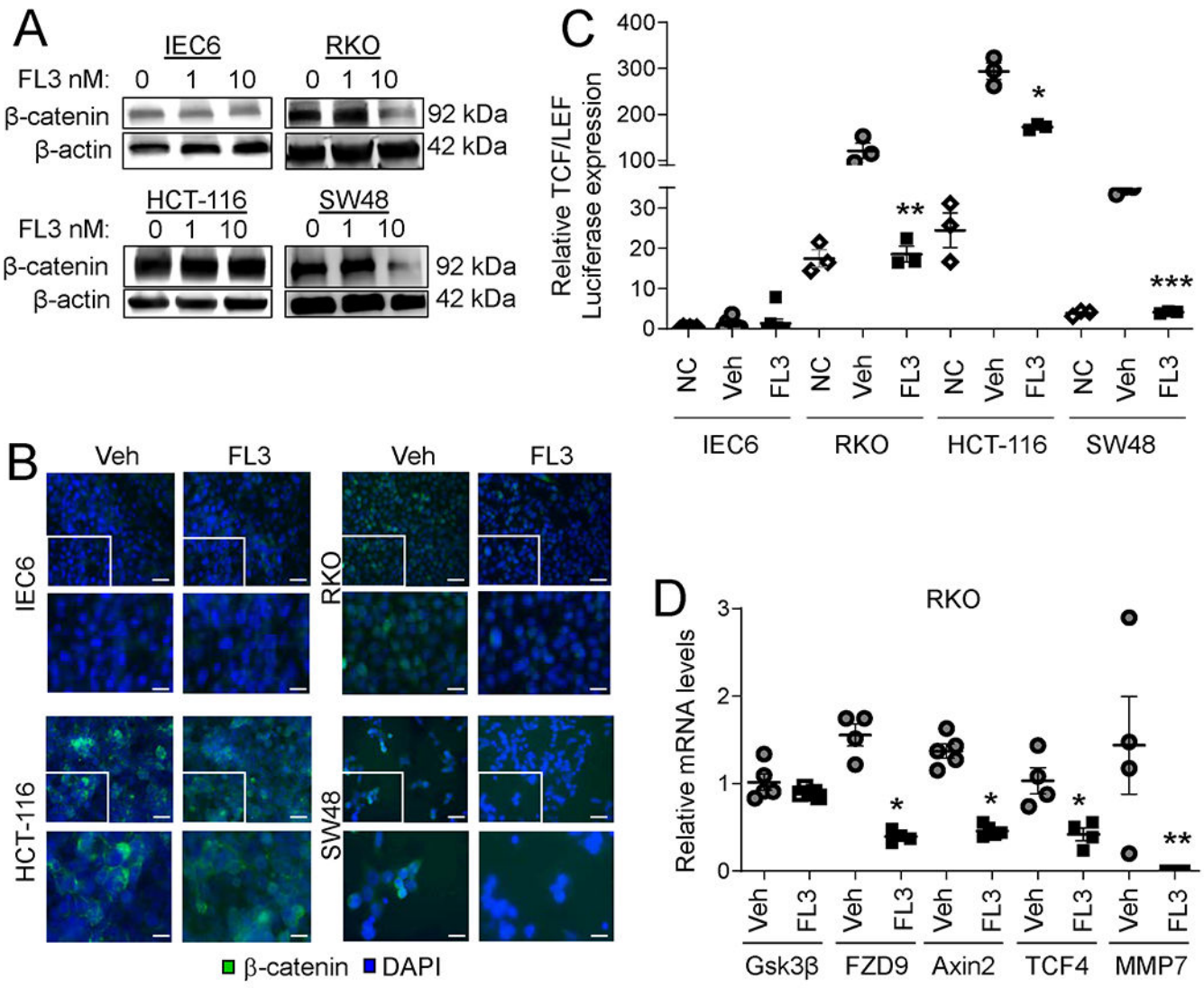

Figure 2. FL3 decreases transcriptional activation by β-catenin and protein expression in RKO and SW48 cells.

IEC6 (normal intestinal epithelial cells), RKO, HCT-116, and SW48 (CRC cells) were treated with 10 nM FL3 for 16 h. (A) Total β-catenin by western blotting. (B) Immunofluorescent staining for β-catenin. Scale bars: 100 μm, boxed pullouts: 50 μm. (C) Relative luciferase expression of transcriptional activation by β-catenin. Negative control (NC) cells were transfected with a non-inducible firefly reporter construct. n = 6 for IEC6, n = 3 for all other cell lines. (D) Relative mRNA expression of Wnt target genes in RKO cells. $*P < 0.05$ vs. vehicle by one-way ANOVA followed by Bonferroni's test. n = 4-5 after outlier removed by Grubs test. $***P < 0.005$, $**P < 0.01$, $*P < 0.05$ vs. vehicle by one-way ANOVA followed by Bonferroni's test.

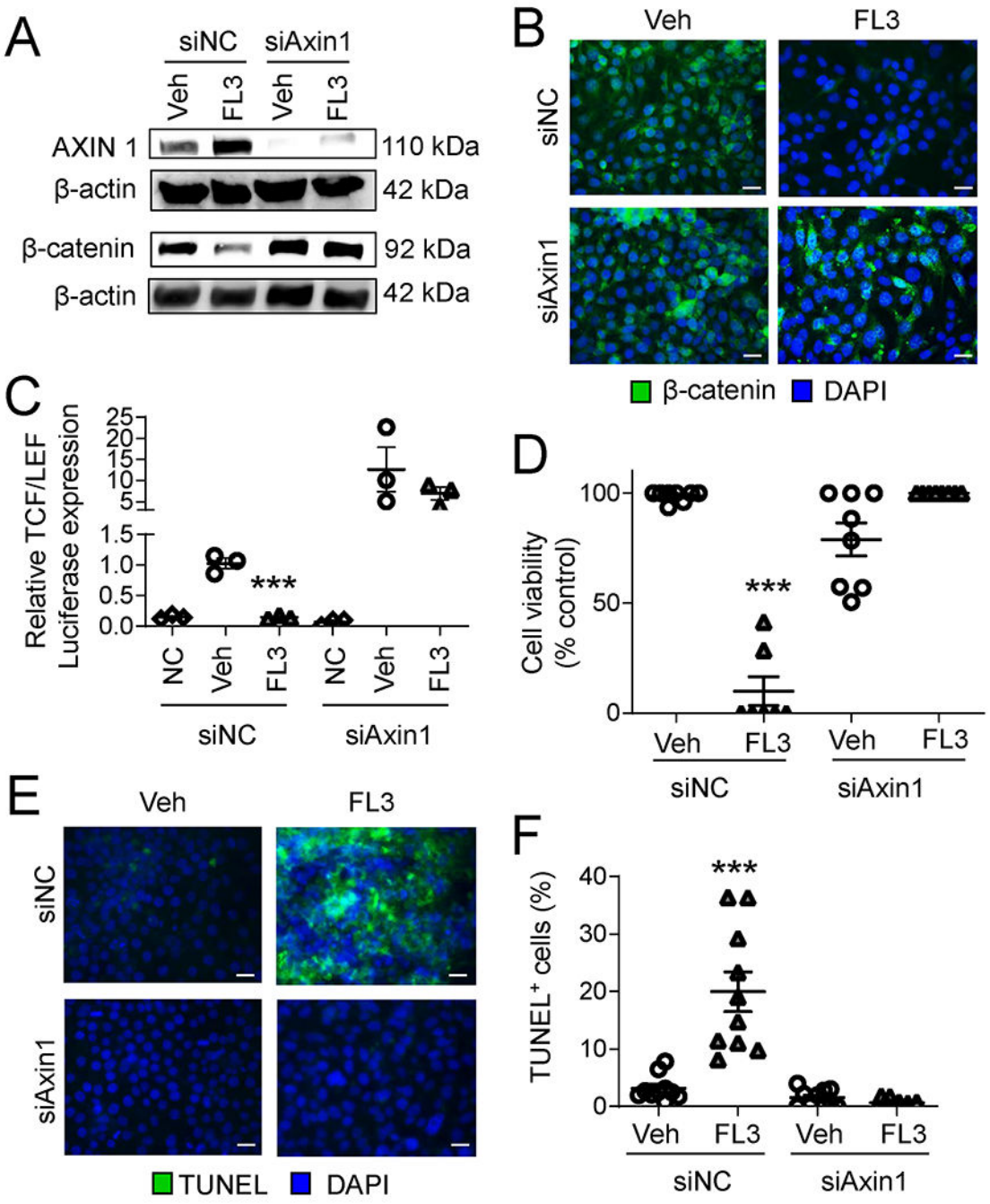

Figure 3. FL3 inhibition of Wnt/β-catenin and induction of cell death in RKO cells is dependent on Axin1.

RKO cells were transfected with three pooled unique siRNA duplexes against Axin1 (siAxin1) or RNAi non-specific negative control (siNC) for 48 h and then treated with 10 nM FL3 for 16 h. (A) Representative western blots to validate efficiency of Axin1 knockdown and effect on β-catenin protein expression. (B) Immunofluorescent staining for β-catenin. Scale bars: 100 μm. (C) Relative luciferase expression of β-catenin transcriptional activation. Negative control (NC) cells were transfected with a non-inducible firefly reporter construct. n = 3 in 2 independent experiments. (D) Cell viability measured by LDH release.

n = 8 per group. (E) TUNEL immunofluorescent staining. Scale bars: 100 μm. (F) % $TUNEL^+$ cells per field, 10 fields quantitated and averaged across 10 wells. ***$P < 0.005$ vs. vehicle siNC by two-way ANOVA followed by Bonferroni's test.

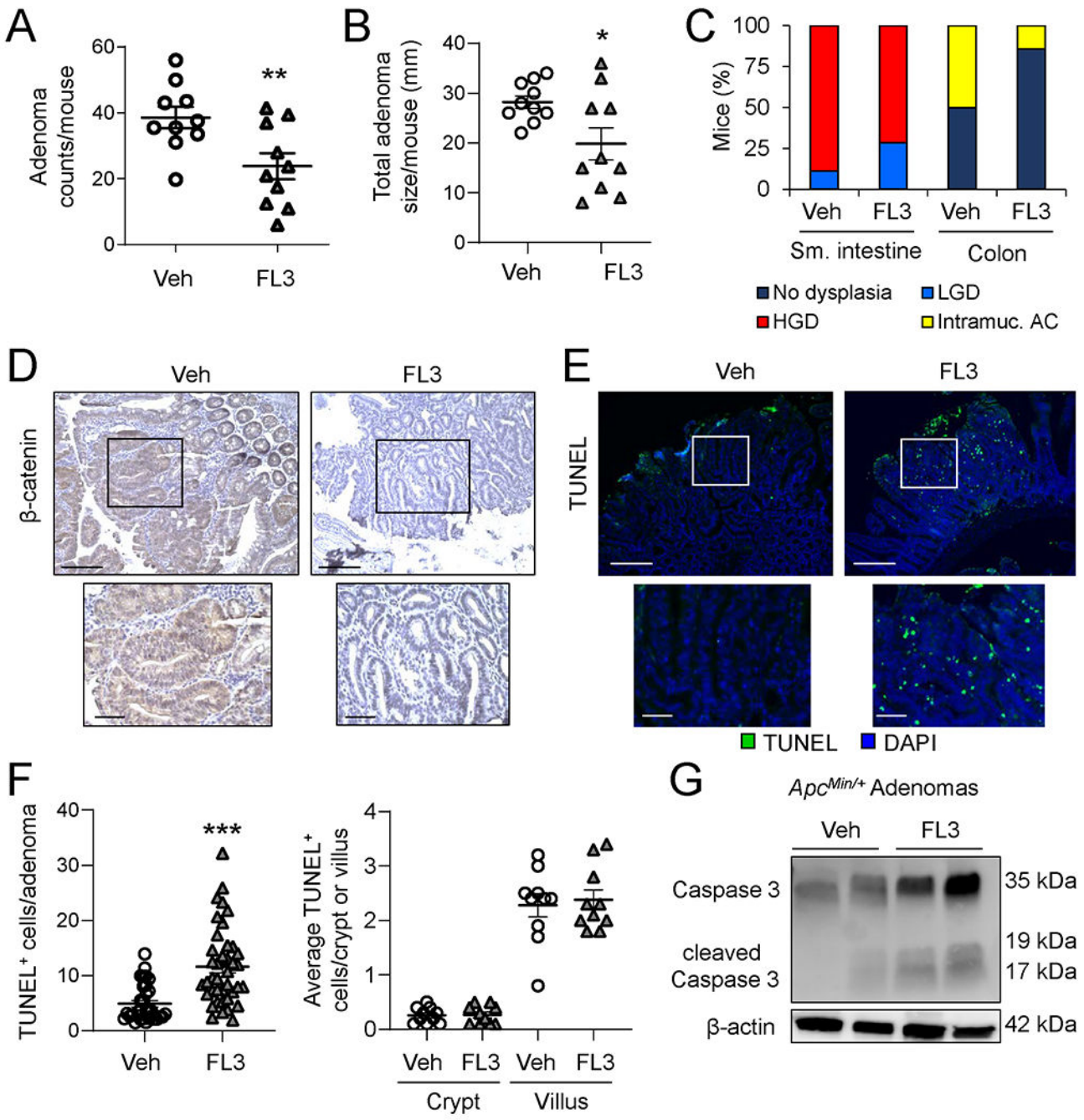

Figure 4. FL3 decreases intestinal tumorigenesis in *Apc*$^{Min/+}$ mice.

Beginning at 15 weeks of age, *Apc*$^{Min/+}$ mice were i.p. injected with 0.1 mg/kg FL3 of vehicle twice weekly for 5 weeks. (A) Average adenoma counts per mouse. (B) Average adenoma size per mouse. (C) Percentage of mice displaying highest extent of dysplasia. (D) Immunohistochemistry staining of β-catenin in adenomas. (E) TUNEL immunofluorescent staining in adenomas. Scale bars: 250 μm, boxed pullouts: 50 μm. (F) Quantification of TUNEL^{+} cells per adenoma, crypt, or villus. (G) Western blot of apoptosis marker cleaved

Caspase 3 from total protein of isolated adenomas. n = 10 mice per group. *$P < 0.05$, **$P < 0.01$, ***$P < 0.005$ by unpaired, two-tailed Student's *t* test.

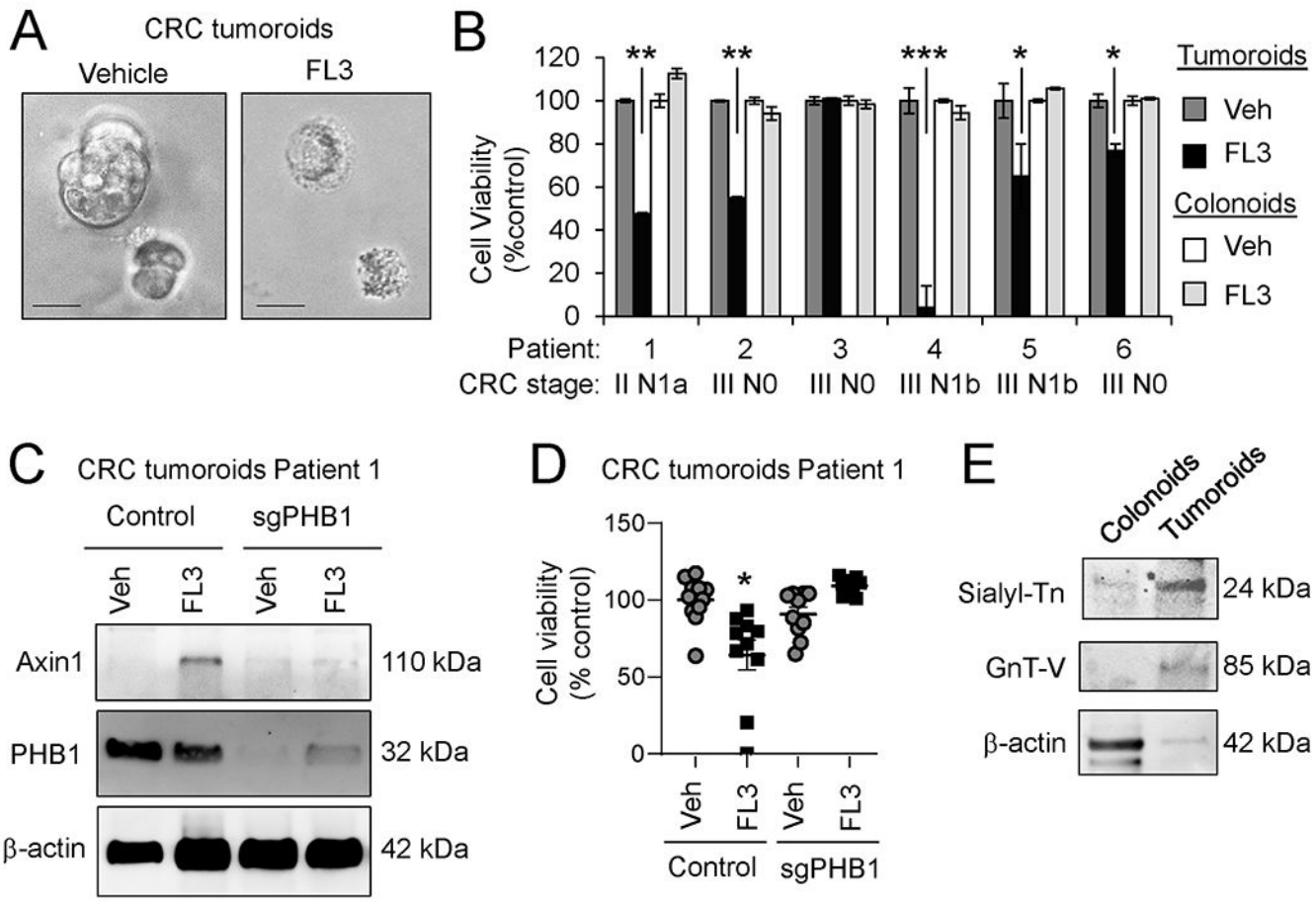

Figure 5. FL3 decreases viability of human CRC tumoroids but not matched-normal colonoids.

(A) Light microscopy of tumoroids derived from stage II N1a CRC demonstrates that FL3 disrupted morphology indicative of dead cells. Scale bars: 100 μm. (B) Cell viability was measured by LDH release from CRC or matched-normal colonoids from 6 patients treated with 50 nM FL3 for 16 h. $*P < 0.05$, $**P < 0.01$, $***P < 0.005$ vs tumoroid veh by one-way ANOVA followed by Bonferroni's test. n = 6 wells per treatment. (C-D) CRC tumorids derived from Patient 1 were dissociated into single cells, nucleofected with CRISPR-Cas9 sgRNAs targeting *PHB1*, and 72 h later treated with 50 nM FL3 for 16 h. (C) Efficiency of sgPHB1-targeting and Axin1 protein expression measured by western blotting. (D) LDH release. (E) Western blots of glycocalyx markers in human colonoids and tumoroids from Patient 1. $**P < 0.01$ vs control veh by one-way ANOVA followed by Bonferroni's test. n = 10 per treatment.

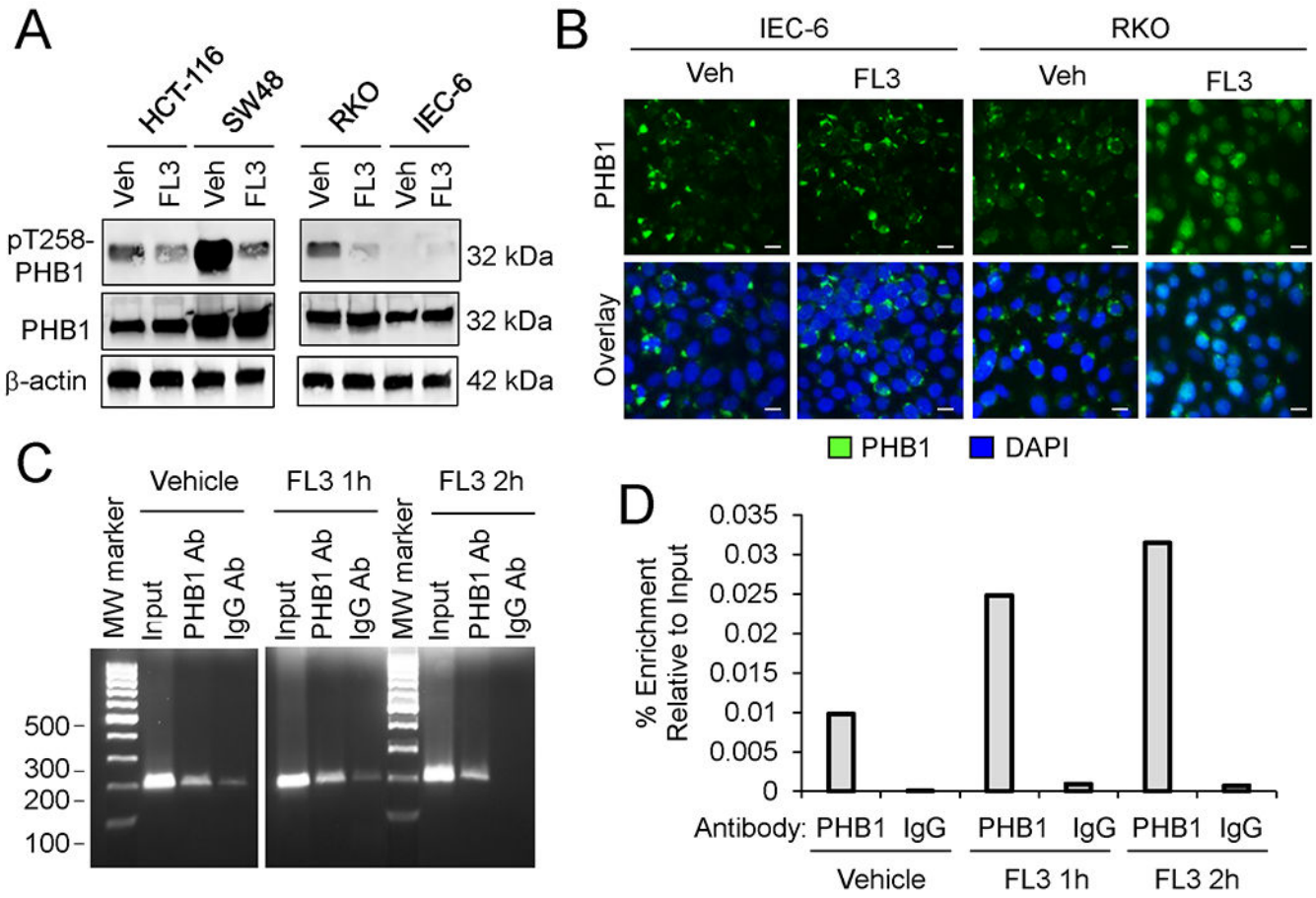

Figure 6. In CRC cells, FL3 blocks phosphorylation of T258-PHB1 and induces nuclear translocation of PHB1 where it binds to the promoter of *Axin1*.

(A) Western blot analysis of cells were treated with 10 nM FL3 for 2 h. (B) CRC RKO cells and normal IEC-6 epithelial cells were treated with 10 nM FL3 for 2 h. Immunofluorescent staining of PHB1. (C-D) Chromatin was isolated from RKO cells treated with vehicle or 10 nM FL3 for 1 or 2 h. ChIP assays were performed using PHB1 or IgG control antibodies and primers spanning the putative PHB1 binding site in the *Axin1* promoter. Immunoprecipitates were analyzed by PCR (C) and qPCR amplification (D) to show the relative enrichment of PHB1 binding as percentage of total input DNA.